Exploring the Spatial Economy by Night

Bergs, Rolf

12 February 2016

Exploring the Spatial Economy by Night

Rolf Bergs

Exploring the Spatial Economy by Night

Rolf Bergs[1]

1. Introduction

Night satellite images may offer an interesting tool to generate socio-economically relevant data and to analyse the evolution of space, e.g. cities or rural areas, and how spatial units interact over time. This paper is just an essay with preliminary ideas for discussion; the approach is explorative-methodological rather than one putting an empirical focus on a defined research item. Empirics discussed in this paper are just various examples collected from tinkering.

Henderson et al. (2003) found that there is a significant association between economic growth and the emission of visible light (in the wavelength range between 380 - 700 nm). Mean correlation coefficients between luminosity and GDP (PPP) calculated by Chen and Nordhaus (2011) are stable at slightly more than 0.8 with a minor standard deviation of just 0.009 (Chen and Nordhaus 2011, annex, p.11). The connection between both variables is energy consumption for public utilities, communication, production and settlements that all needs light. The advantage of visible light emission is its one-dimensional scope of data generated: There is only a range between black, the different grey shades and white, while daytime images gives one some idea of settlement, commercial, green and traffic zones with a high variation of colours with different brightness that are hard to translate into meaningful raw data.

A major purpose of using night satellite images for economic analysis has been the search for proxies for production and population density in countries with insufficient and unreliable data infrastructure. This essentially applies to less developed countries where weak data infrastructure is often part of overall underdeveloped administrative capacities. Hence, there was the idea to estimate important social and economic profiles of such countries and regions by the luminosity proxy and to improve the decision base for policies and aid. [2]

The fundamental assumption is that there is not only a significant empirical relationship between luminosity and income (or labour productivity respectively) and luminosity and population, but that error in both, luminosity and socio-economic data, is independent. The latter assumption is even more important than the former:

> "…In general, a positive correlation between measured income (national accounts or survey means) and nighttime lights could be due to two factors: that they are both correlated with true income, or that their measurement errors are strongly correlated

with each other. However, the latter possibility is implausible because the generating process of nighttime lights data is to a very large degree independent of the generating process either of national accounts or of survey means. For example, measured income is collected by statisticians interacting with survey respondents, while nighttime lights are recorded impersonally by satellites…" (Pinkovskiy and Sala-i-Martin 2014, p. 2).

Light emission is essentially a by-product of production and consumption (cf. Henderson et al. 2003). The brightness of nocturnal light reveals the density of human activities. Error variance of luminosity is rather constant around the globe while there is a large variation of error for datasets in official social and economic statistics. In many developing countries the error variance of official statistics is higher than that of light emission, while in industrialised and newly industrialised countries official data are more reliable so that further satellite data on luminosity would not add value. That is the reason why night satellite analysis is of relevance for developing countries rather than for industrialised ones (Henderson et al. 2008, Chen and Nordhaus 2011). However, this differentiation only holds for purposes to derive proxies for production or population data. In fact, there is also reason to use this tool in the observation of (spatial) economic patterns and trends in the more industrialised countries. Spatial distribution of rural areas, urban agglomerations, border areas or other spatial categories are to be mentioned. Interesting indicators such as changing border effects, growing peri-urban zones, trends of polycentric or monocentric development or the rank size distribution of settlement clusters can be made visible and processed by using night satellite images.

Just comparing normal geographical maps is insufficient to shed light on urban and rural change. Enriching topographic or political maps with external data (GIS) helps to monitor spatial change by variables for which data are available. This is, however, only possible at a higher administrative level, such as countries, regions and - to a limited extend - districts. Thus, by using official statistics the view on space is truncated. Micro-spatial patterns and processes cannot be observed that easily, even though there is a growing literature on using micro-spatial raster data for the research on neighbourhood effects viewed from different perspectives, such as labour market, education, migration, investment choice and others (e.g. Halleck Vega and Elhorst 2002, Zwiers et al. 2014, Coulter et al. 2015, Duranton and Overman 2002).

2.   *Spatial heterogeneity, spatial dependence*

The night satellite images may provide an opportunity to explore patterns of spatial dependence (e.g. how space is influenced by further contiguous or distant space) and spatial heterogeneity (e.g. how attributes of space are distributed, whether there are regular or irregular patterns). In econometric modelling with a spatial relation, both features are of major relevance to consider, when it comes to efficient estimates. Two *Gauss-Markov* assumptions are to be acknowledged, namely the non-constant variance of variables over space and the covariance between observations at different places. Consequently, heterogeneity and dependence can be conceived also as stand-alone categories to describe

and analyse space. Spatial dependence and spatial heterogeneity are both results of processes; while heterogeneity is the result of a deterministic process and cause of a further continuing process, spatial dependence is rather a stochastic process in which spatial variables in one territorial area are influenced from other contiguous or distant areas. In practice, spatial dependence and heterogeneity can be conceived as follows:

Spatial heterogeneity is related to the variation of relationships over space. It is thus a property describing the uneven distribution of variables describing space, such as population, topography, economic assets etc. If the world were a fully homogenous space, there would be no need for transport because every point of space would be identical such as in a closed vacuum. Cities side-by-side with rural areas, different levels of population density, converging and diverging regions or simply maritime versus continental climate areas are indications of spatial heterogeneity. But the concept of spatial heterogeneity also comprises a more holistic view on spatial structures, often based on fractal geometry such as multi-scalar global patterns that come close to natural laws, like the *Zipf* law of rank-size distribution of cities or the forms of coast lines or topographic reliefs. The concept of "natural cities", their detection by nighttime imagery and the subsequent estimation of their characteristic distributions is an example for that (Jiang 2014).

Spatial dependence in a sample dataset means that observations on a variable *k* at a location *i* are not independent from observations *k* at other contiguous or more distant locations *j≠i*. A central attribute of spatial dependence is the covariance of selected random variables over space: While spatial heterogeneity represents the first-order moments of space, spatial dependence is traditionally conceived as a second-order property.[3] Spatial units influence each other to a varying extent – primarily depending on distance, markets, politics and social fabric. An indicator of spatial dependence is spatial autocorrelation. In spatial econometric modelling it is considered either by spatial autoregressive or spatial error models (see footnote 4 below). But spatial autocorrelation can be also used as a stand-alone indicator for descriptive statistical analysis. This way, the *Moran-I* coefficient (in analogy to the *Pearson-r*) or the *Geary-c* coefficient are measures of estimating spatial dependence. (Anselin 2001, Le Sage 1999)

3. *Further literature*

Meanwhile there is growing literature dealing with economic research based on night imagery. While Henderson et al. (2003), Chen and Nordhaus (2011) and Sutton et al. (2007) primarily deal with the examination of light emission as a proxy for missing economic and social data (most importantly production and population). Mellander et al. (2011) examine

---

[3] Even though, there are arguments that the relationship is contrary, namely that spatial heterogeneity is rather a second-order effect, while dependence is the first-order one. Jiang (2014) argues that "…Spatial heterogeneity is a kind of hidden order, which appears disordered on the surface, but possesses a deep order beneath. This kind of hidden order can be characterized by a power law or a heavy-tailed distribution in general. …". So if just viewing the visible heterogeneity at the surface, then the dependence between spatial items is a higher order effect, but if looking at underlying regular patterns of heterogeneity, spatial dependence constitutes a lower (first) order effect.

the explanatory power of night imagery specifically for economic activity rather than economic growth, population density or urbanization for Sweden. Ghosh et al (2010) used the night imagery to develop a method to identify informal economic activity that is not recorded in official statistics. Pinkovskiy and Sala-i-Martin (2015) examine whether GDP per capita recorded in national accounts or mean income and consumption data from household surveys are better proxies for income in linking the evolution of both series to the change of night image luminosity. Pinkovskiy (2013) looks at discontinuities of the political economy along borders using a regression discontinuity design. Border discontinuities are supposed to shed light on the impact of the political economy on economic activity because these determinants are produced by government activity. Luminosity per capita and its change over time behaves discontinuously upon crossing a border from a poorer (or lower-growing) into a richer (or higher-growing) country. According to Pinkovskiy these discontinuities seem to form lower bounds for discontinuities in economic activity across borders, which suggest a major importance of national-level variables such as institutions and culture relative to local-level variables.

There are several further studies linking night imagery and socio-economic variables – the majority on developing countries - but there are only rather few (e.g. Jiang 2014, Jiang et al 2015, Liu 2014) using the night imagery to shed light on spatial dependence and spatial heterogeneity, both of major relevance in spatial economics.

4. *Images*

The images analysed in this paper are satellite images of the National Oceanic and Atmospheric Administration (NOAA):.

Global nighttime lights imagery data are collected by the Defense Meteorological Satellite Program Operational Line Scanner (the DMSP-OLS Nighttime Lights Global Composites - Version 4 1992-2010). Several DMSP-OLS image categories that are useful for spatial analysis are freely accessible on the internet. The night imagery data have a spatial resolution of 30 arc-seconds and are recorded between 75°N and 65°S with non-radiance-calibrated light intensity in a Digital Number (DN) range between 0 to 63.

The DMSP-OLS is capable to record and observe light sources in a range between visible-near infrared emissions and strong luminosity, present at night on the Earth's surface, including settlements, roads, gas flares, ships and fires.

The available so-called "products" of imagery are coverage, average visible band values, stable light and average light normalized.

In our examples below we used the average digital number of lights multiplied by the percent frequency of light detection (avg_lights_x_pct). These images are normalised for variations of cloud cover and thus account for the persistence of lights, but one can also test images with stable lights or average visible light.

5. Estimation error

Background noise of night imagery (moonlight reflection etc.) can be filtered out by setting empirical thresholds based on visible light identified in areas with no source of light emission. But due to variation of light emission it is difficult to precisely filter out over-glow. If one looks at the distribution of light emission on the satellite images it is intuitively clear, that a bright area is not illuminated by light from this area alone but also beamed at from neighbouring space and *vice versa*. As Doll (2008) shows, "…a feature of the data acquisition process is that there is a large overlap (some 60%) between pixels. This means that light observed in one location has the chance to be recorded in more than one pixel. This can contribute to a larger lit-area being detected than is actually the case…" (p.12). In a spatial regression analysis average luminosity of a small area depends on light emitted in that area and – to some extent - from contiguous areas[4]. The larger the areas regarded, the less will be the spillover impact from over-glow.

Apart from that it is important to stress the fact that light emission in its association with economic variables is also affected by further sources of error. Comparing population density across countries by using the luminosity proxy will be misleading in many cases, simply because of lower levels in light emission in developing or emerging economies. Ghosh et al. 2010 point out that e.g.

> " … countries such as Japan and Germany are much wealthier relative to their sum of lights value; on the other hand, Russia is much poorer relative to its sum of lights value. …" (p. 153)

At micro- or meso-scale specific land use of economic activity may have an influence on light emission after dark. Henderson et al. 2010 mention the example of the cities Las Vegas vs. Salt Lake City, or the fact that high density multi-storey buildings emit relatively less light compared to flat buildings. Hence, even though there is a significant correlation between luminosity and production over space, it would be rather misleading to use luminosity as a general proxy for missing GDP data, especially for partial analyses with lower numbers of observation.

In addition, different satellites with different technology levels may generate images that are not completely comparable over time, just as a sampling variation due to physical factors. The available OLS images are not inter-calibrated. Inter-calibration of images is important for time series analyses, where systematic breaks through changes of satellites and technology distort the data. In our paper we just compare images at two distinct points of time, hence for the purpose of simplicity, in this paper the simple use of the raw OLS images is deemed justified[5].

---

[4] However, spill-overs are also to be considered for larger areas if visible luminosity m is further related to other variables, such as population, labour productivity or other predictors X, more formally: $m = \rho Wm + \beta X + \varepsilon$, where W is a weighting matrix defining contiguity or distance respectively and ε the error term in a spatial autoregressive model. In an alternative spatial error model the specification would be: $m= \beta X+\varepsilon$, where $\varepsilon= \lambda W\varepsilon+\upsilon$

[5] Liu (2014) presents a method for image inter-calibration (p. 28 ff.). Chen and Nordhaus (2011, p.3) have estimated the standard errors of visible light emission on the DMSP-OLS images by regressing luminosity on GDP Mean standard errors of estimates

6. *The Software ImageJ*

Standard of spatial analysis of maps and geographic images is ArcGIS, a powerful, costly but also rather complex software for geographical analysis, including image analysis. For the analysis of night imagery, pure image analysis software is in most cases sufficient. ImageJ is a widely used open source image analysis software that had been developed by Wayne Rasband at the National Institutes of Health since the end of the 1990s (Schneider et al. 2021). Its primary purpose has been to process images in medical and biological sciences where has obtained a *de facto* standard for image analysis. However, ImageJ as a processing and data analysis toolbox, written in Java, has a broad range of applications - beyond microscopy and medical imaging - such as astronomy[6], environmental analyses[7], earth sciences including remote sensing[8], material sciences[9], viticulture[10] archaeology[11] and others. The software has been permanently further developed. The most powerful feature of ImageJ is its international community with innumerable contributions consisting of plugins and macros. Several tools originally developed for medical imaging are also useful for remote sensing and the analysis of spatial change.

ImageJ is capable to display, print, edit, analyse, process and save images with 8-bit, 16-bit and 32-bit graphic formats. It can read various file formats, such as tiff, bmp, jpg, gif and others. The software allows to calculate area sizes and performs a large range of statistical and mathematical procedures on pixel values and their distribution either globally or in defined selections of any shape. With numerous processing functions such as contrast manipulation, sharpening, smoothing or filters, it is possible to visualize relevant parts of the images. Density histograms and profile plots are examples of statistical diagrams generated. Basic parameters of statistical analysis are mean values and spread but it is also possible to run more sophisticated analyses starting from image correlation to detecting fractal structures. It is easy to import the numeric data in statistical packages like R or Stata in order to merge datasets and to run further statistical of econometric procedures. The package is therefore also widely used as a Remote Sensing software. Distances and angles can be measured. Even though the software is not geo-sensitive itself it is possible to calibrate geographical images containing geo-reference by figure calibration.[12] In the numeric dataset of moments the geographic coordinates can be saved and further processed.

---

for luminosity between the four different satellites, on the one hand, and for one satellite over years, on the other hand, are found by Chen and Nordhaus in the range between 0.3 and 0.6 with a decreasing trend over time for 1°x1° grid cells (Chen and Nordhaus 2011, annex, p. 9).

[6] West and Cameron 2006; Damas et al. 2014
[7] E.g. van Woesik et al.; Troscianko and Stevens 2015
[8] E.g. Berra et al., Buntilow 2013
[9] E.g. Ushizima et al
[10] Whalley and Shanmuganathan 2013
[11] Verhoeven et al. 2013
[12] Geographic images are usually geo-referenced in a geo-tiff format. Even though ImageJ itself does not process and save the geo-referencing information it is possible to calibrate the image with the frame coordinates by the plugin "Figure Calibration". As long as the image is open, any analysis – also of parts cropped to a new image file – can be done. The subsequent numeric analysis can be collated to the frame coordinates.

7. *Examples of spatial analysis with ImageJ*

7.1 Selection

ImageJ comprises a variety of area selection tools. The simpler ones are point and multi-point, rectangular, elliptical, polygon, freehand and straight line selections. These are part of the core software with button commands or commands from the pulldown menu. However, there are several further more complex selection tools provided as plug-ins or macros. Powerful plugins are e.g. the application of concentric circles or the radial profile. It is also possible to write macros for different individual kinds of selection (see below).

7.2 Partial analysis

A major advantage of the night satellite images is independence from official data and administrative boundaries. It is possible to define the partitioning of a map at the discretion of the researcher. The easiest tool of partial analysis is simply to crop the map and to focus the analysis on a defined section. Within the defined section it is then possible to select further sub-parts. In using the command "restore selection" the selection of an image at t_0 can also be copied to the same image at t_n. In comparing results of alternative partitioning it is possible to run various (infinite) sensitivity analyses. This can be very interesting for analyses of spatial change and spatial dependence such as spatial autocorrelation analyses. One possible approach could be to select sub-regions by free-hand (e.g. according to administrative boundaries); another approach can be to subdivide a map into raster cells, e.g. square kilometers[13]. This can be easily realized by writing simple ImageJ macros like the following one:

```
x = 0;
y = 0;
width = 1.785714286;
height = 1.785714286;
spacing = 0;
numRow = 100;
numCol = 100;

for(i = 0; i < numRow; i++)
{
        for(j = 0; j < numCol; j++)
        {
                xOffset = j * (width + spacing);
                print(xOffset);
                yOffset = i * (height + spacing);
                print(yOffset);
                makeRectangle(x + xOffset, y + yOffset, width, height);
                roiManager("Add");
                if (roiManager("count") > 10000)
                        {
                        print("Maximum reached: 10000 entries have been created.");
                        exit;
                        }
        }
}
```

---

[13] The maps of DMSP-OLS are scaled to one pixel = 0.56 kilometers

Moments of such raster cells (either in total or selected cells) can be further processed and subsequently analysed by statistical procedures, either by ImageJ itself or statistics software. The smaller the cells the more it is possible to delineate administrative units by raster cells. It is then possible to add up different raster cells and compare the selected units over time.

The following example shows a selected raster (1x1 kilometer cells) of the Frankfurt region taken from the 1992 image:
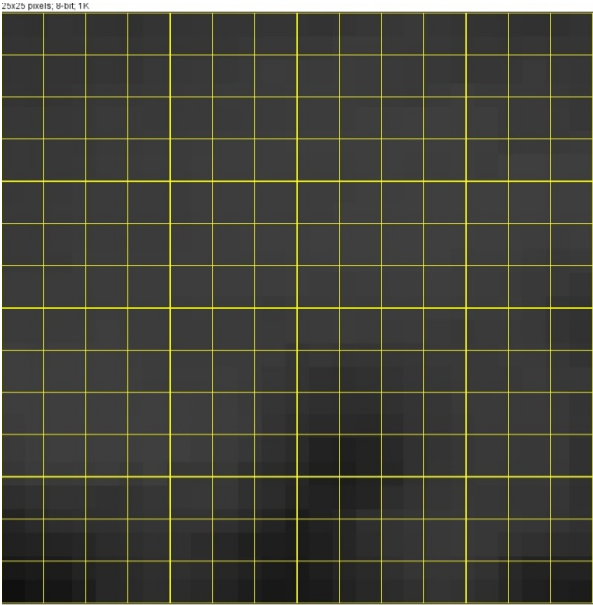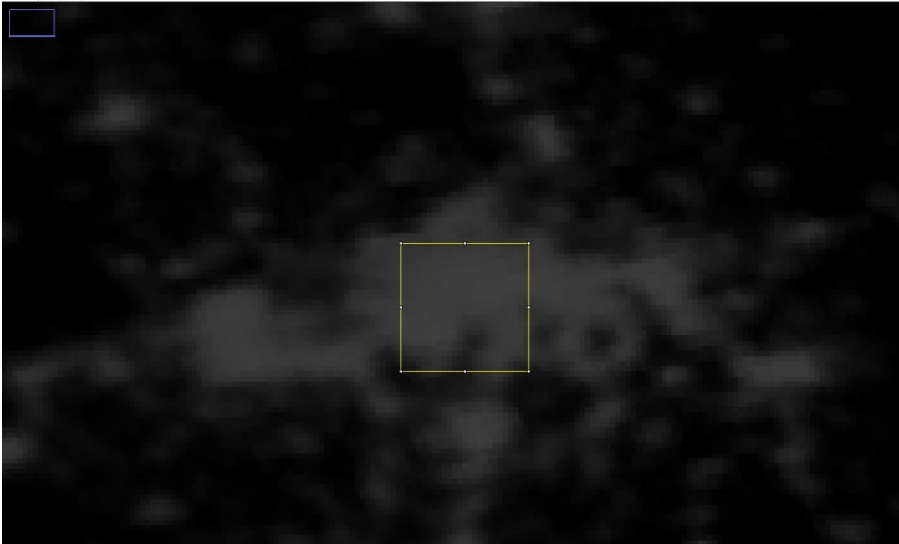
In chapter 8 examples of further selection procedures and statistical analysis are discussed.

7.3 Visual inspection

One, perhaps even the most powerful tool of the maps is simply the image itself. The following night satellite image with a medium transparency shows the Korean peninsula. The northern and the southern part are immediately visible by a discontinuity of light emission exactly along the political border between both.

Satellite image from: DMSP-OLS Nighttime Lights Global Composites (Version 4): Snapshot of the Korean peninsula in 2010

In many cases, the information provided by the first glimpse at the image already contains the main message. Statistical analysis is then only needed to verify or falsify the estimate from visual inspection.

7.4 Statistical analysis of images

Comparative analysis of night images may shed light on spatial change, like urbanization or economic integration processes. The former is visible around cities, while the latter notably along administrative boundaries like national borders. With a simple image correlation analysis it is possible to view the variance of the pixel-by-pixel DN at two or more points of time. A high correlation coefficient (*Pearson's r*) will indicate either a little or a very balanced change so that all pixels change their intensity with roughly the same rate. If there is a stronger urbanization process over time, image correlation will be lower, because there will be a certain portion of black pixels becoming grey or white while also many formerly black pixels remain black. Then the more the regarded city is zoomed in, the lower the image correlation coefficient will be.

More insight into patterns of spatial dependence will be provided by the analysis of spatial autocorrelation. Visual inspection of the night images reveals that both, areas with high and higher luminosity as well as those with zero and low luminosity are clustered and that between both types of areas there is smooth transition. It is unusual that pixels with DN=63 are side-by-side with zero pixels[14]. This shows that spatial units are not independent from neighbour units. However, the level of global spatial dependence of an area or local spatial

---

[14] This is even unusual for untenable areas because of the over-glow effect (cf. the images of Tripoli that contain brighter pixels that are in fact located in the Mediterranean Sea).

dependence between neighbouring units within an area may change over time. Areas close to a city that were formerly rural may have attracted investment into production or housing showing a peri-urbanisation process that is indicated by higher luminosity, similar to that of the city itself. Rural areas become functional for the metropolitan area of a city, and spatial dependence will thus increase. Such a process can be indicated by a comparative analysis of spatial autocorrelation using the *Moran's I* coefficient.

$$I = \frac{N}{\sum_i \sum_j w_{ij}} \cdot \frac{\sum_i \sum_j w_{ij} (X_i - \bar{X})(X_j - \bar{X})}{\sum_i (X_i - \bar{X})^2}$$

where N is the number of observations and w the weight specified in a contiguity matrix.

In an evolution of functional areas spatial autocorrelation would indicate higher integration of urban and former rural areas. Declining spatial autocorrelation would indicate the opposite. Further below some examples of such analyses are illustrated.

In the following chapters we discuss some examples ranging from visual inspection to further statistical analysis of images, such as spatial autocorrelation.

8. *Urban evolution from the macro perspective: Urbanisation and Polycentricity vs. monocentricity*

8.1 Urbanisation of the Tripoli region

Urbanisation in more recent times is well visible in countries that have grown rapidly, both in terms of their economy as well as well as in terms of population. The following two images show the North-West of Libya with the agglomeration of Tripoli in 1992 and 2010. A simple tool is just measuring distances of homogenous areas and to compare the results over time.[15] Measuring the distance of the metropolitan extension between the North (Mediterranean Sea) and the South resulted in some 8.9 km in 1992, while in 2010 the lit area strongly extended up to the desert with 27.56 km.

---

[15] ImageJ provides a tool to set scales (here one pixel=0.56 km)
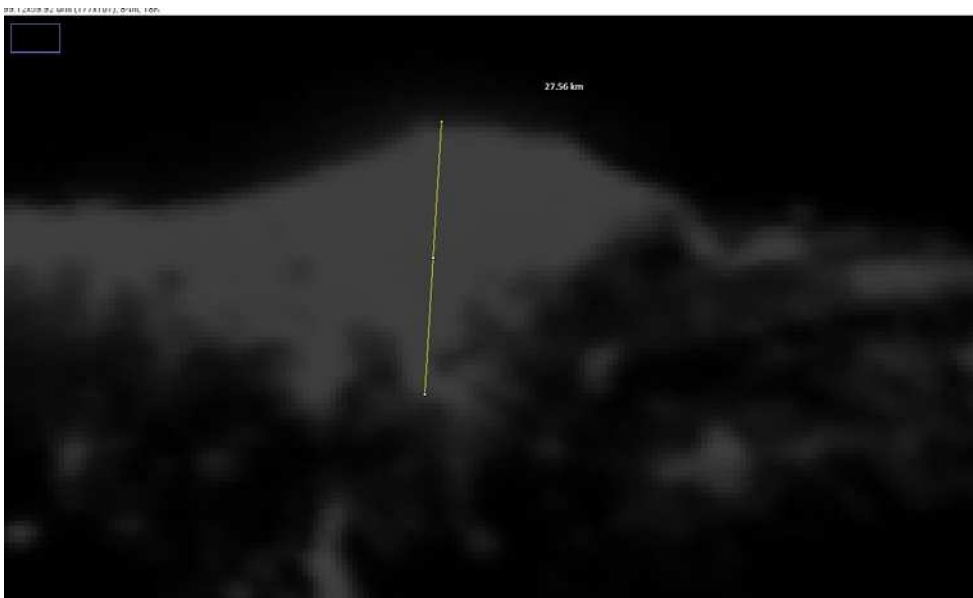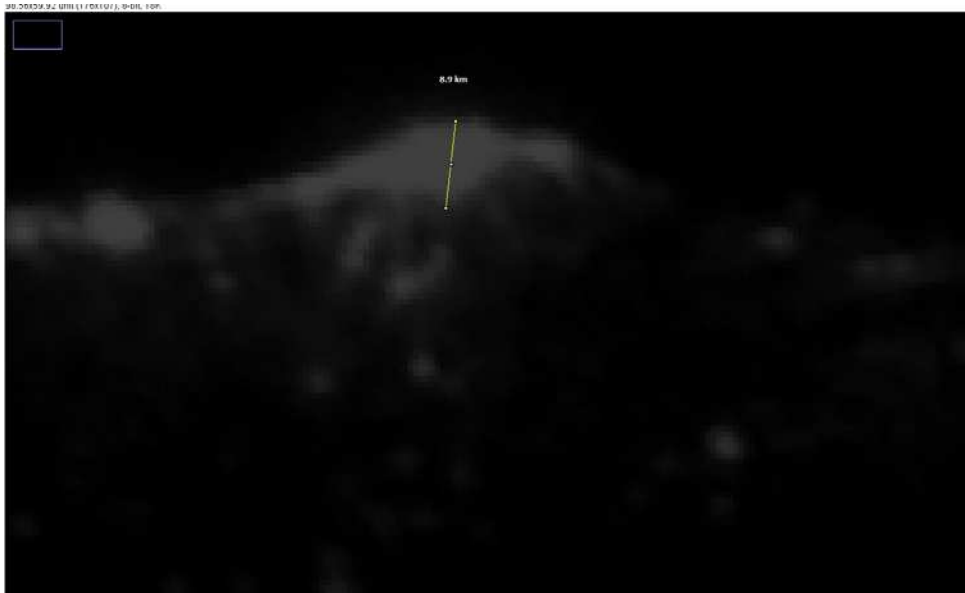
8.2 Is there polycentric development? - The Blue Banana

Another simple tool is filtering in making patterns of images more visible. The following images and surface density plots show the Western European core-periphery pattern (Blue Banana) based on luminosity intensity and visualised by the 5-ramps filter. The green areas show those regions with the highest density of top luminosity (DN=63). These are also the major cities and metropolitan regions. The following two images illustrate clearly the map of Western Europe. Both compared show an increasing trend of urbanization (areas of high luminosity have grown) but no polycentric trend, even though a first glimpse could suggest an impression of a significant polycentric trend. The number of clusters with DN > 60

increased from 387 to just 388; by comparing unit areas with DN=63 there is even a reduction from 169 to 155.[16]
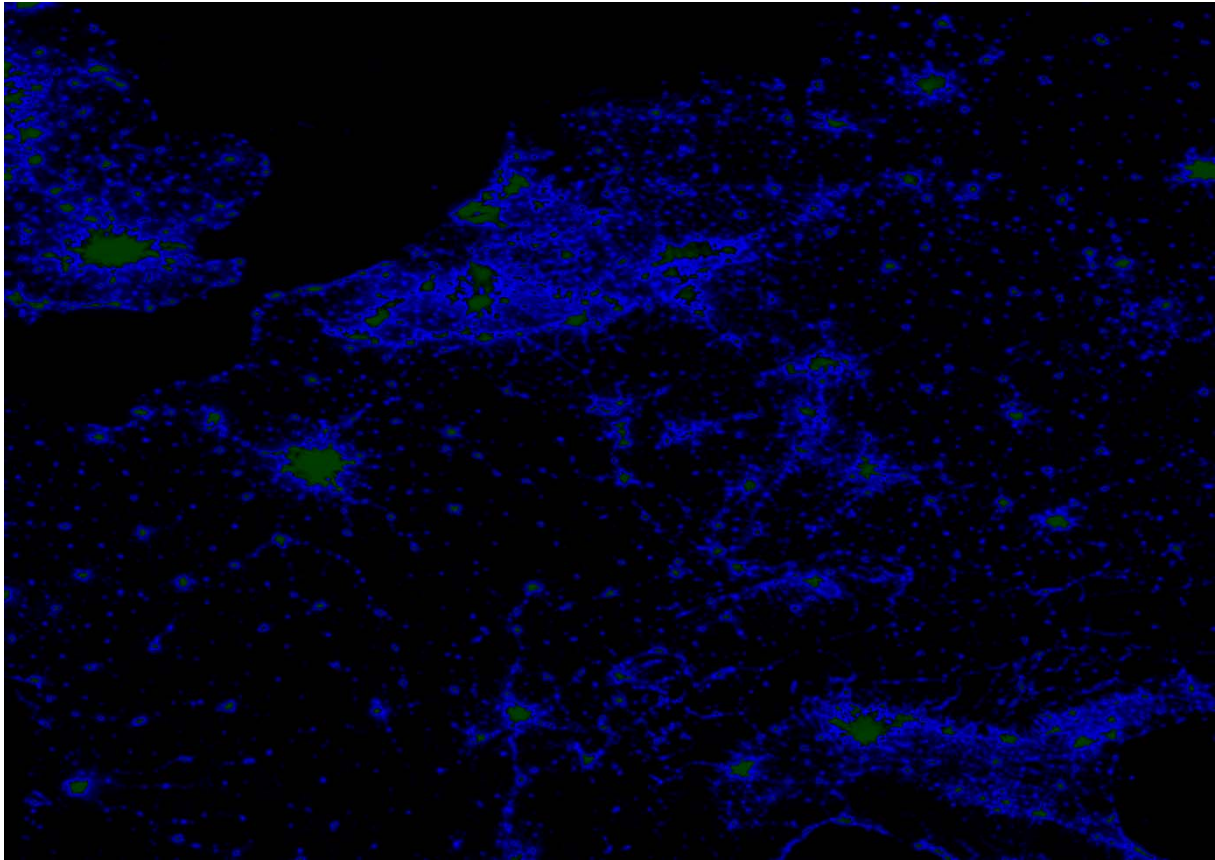
610x519 pixels; 8-bit; 309K
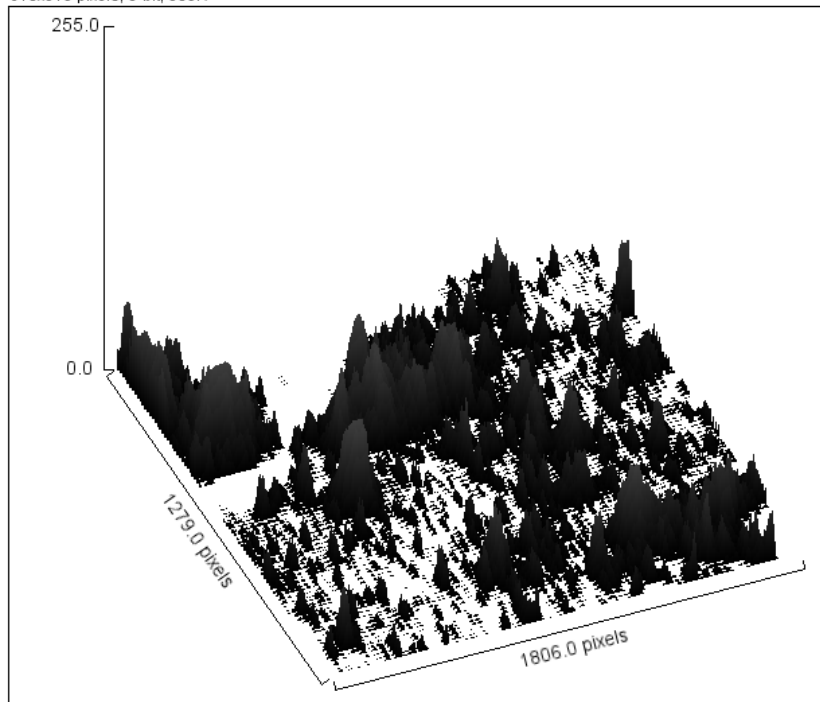
„Blue Banana" 1992

---

[16] Counting clusters is possible by the "Analyse Particles" command. To run this procedure, the image has first to be transformed into a binary image. Then it is possible to set thresholds, e.g.to select only areas with DN>60.

610x519 pixels; 8-bit; 309K

255.0

0.0

1279.0 pixels

1806.0 pixels
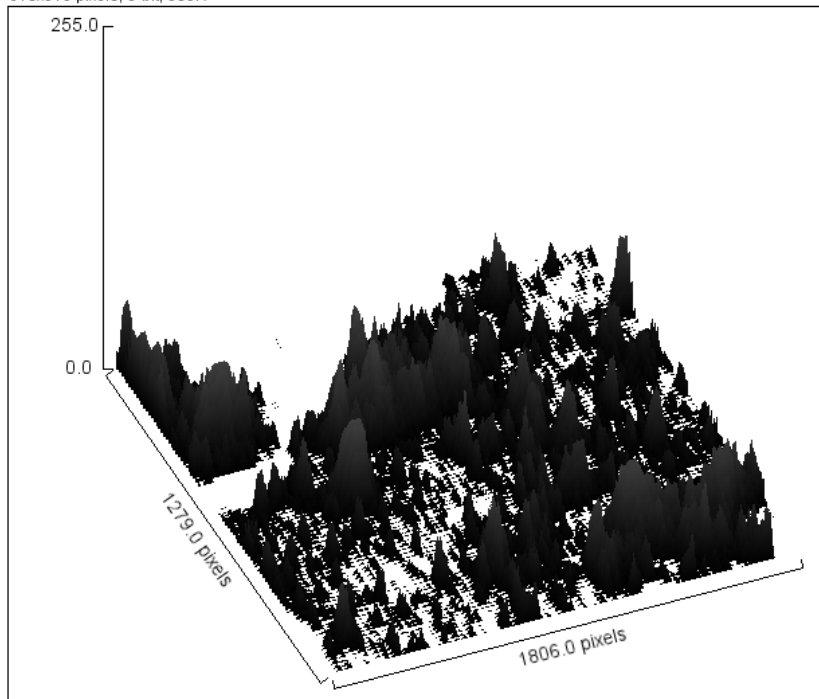
"Blue Banana" 2009

Beyond pure visual inspection it is of course possible to explore such an image also in statistical terms, such as image correlation, spatial dependence, e.g. *Moran-I*, or spatial heterogeneity, e.g. the rank-size distribution (see further below).

9. *City growth and peri-urbanisation – the meso perspective: Examples Frankfurt and Madrid 1992 versus 2009*

Images contain pixels with different levels of brightness. The DMSP-OLS images are in the range between 0 and 63. Brighter parts are more associated with agglomerations (higher population density); parts with little light emission usually indicate rural areas with lower population density. Areas with zero emission are supposed to be sea, lakes, mountains, forests or other untenantable areas. Changing intensity and distribution of light emission may indicate spatial change along the continuum between urban, rural and untenantable parts. The observation of different and changing levels of light emission could also help to overcome the traditional normative dichotomy of the "rural" and the "urban".

9.1 Frankfurt

In the following example we compare the region of Frankfurt in 1992 and 2009. The image shows the wider Rhein-Main area with Frankfurt as its core center. It extends from Gießen in the North to Darmstadt in the South and from Bad Kreuznach in the West to Aschaffenburg in the East (The following descriptive statistics are given by ImageJ:

Descriptive statistics:

Image	Area	Mean	StdDev	Min	Max	IntDen
`Frankfurt1992.v4b.avg_lights_x_pct.lzw-1.tif`	18,832	15.15	16.86	0	63	285,232
`Frankfurt2009.v4b.avg_lights_x_pct.lzw.tif`	18,832	18.63	17.45	0	63	350,861

The images show exactly the same area at the two points of time (during 17 years). The mean pixel DN and the brightness-weighted average of the x and y coordinates of pixels has increased, the standard deviation has remained rather stable.

Image correlation 1992 vs. 2009:

Pearson's_r
0.96

The image correlation is very high indicating either a very little change over that long time period or a very balanced one. The standard deviation remained stable, thus most parts of the area underwent a trend in the same direction. Economic growth has therefore been a spatially balanced process across the area regarded. For comparison, the image correlation of the two images of the Tripoli region (see above) is only at 0.77 indicating a major spatial change over that period.

Spatial autocorrelation over time with concentric circle analysis:

Empirical analysis of urbanization has traditionally based on data from official statistics. A core research question has been: How do municipalities develop in terms of population, production and labour market? Sufficient data at municipal level and below are rare, incomplete and often incomparable across municipalities. Analysis of spatial dependence is thus based on data for spatial entities within their administrative boundaries; boundaries and space are irregular. Connectivity weights are constructed on common borders, length of common borders or distances, but the irregular form of the lines of boundaries make it difficult to select a perfect weighting matrix.[17]

An alternative would be to view spatial dependencies across raster units, e.g. square kilometers (see above the raster selection of Frankfurt) or e.g. – for micro-spatial neighbourhood analyses – hectares.

Usually, cities grow radially, only limited by natural or adminstrative boundaries (like sea, mountains, national borders); areas around cities have various functions, and those functions may change over time. This had been a finding already by von Thunen in the 19th century (the *von-Thunen*-rings). For our purpose it could be thus worth to test spatial dependence across such concentric circles. The major advantage is the directly extractable database (pixel intensity distribution) that is independent from administrative borders and adaptable to more natural paths of city/settlement evolution, i.e. a radiating spatial change. Of course selection of the center, the rings, the number of rings and the choice of the radius is at the discretion of the researcher; on the one hand such selection may appear arbitrary, but on the other hand there is the opportunity of an infinite number of different selection choices, so there is the advantage of numerous sensitivity analyses confirming or questioning a prior hypothesis.

Of course such a concentric circle analysis makes only sense if providing a plausible justification how to position the circles (e.g. city centre + rest of inner city within one versus two circles, separation of outer suburbs and adjacent municipalities, number of circles and decision which circles should be unified to one, different sets for sensitivity analyses etc.).

The following analysis is only a simplified example:

---

[17] Apart from that, other non-geographical forms of connectivity also influencing spatial dependence are not sufficiently considered (cf. Beck et al 2006).

Night Satellite Images: Frankfurt 1992 and 2009:
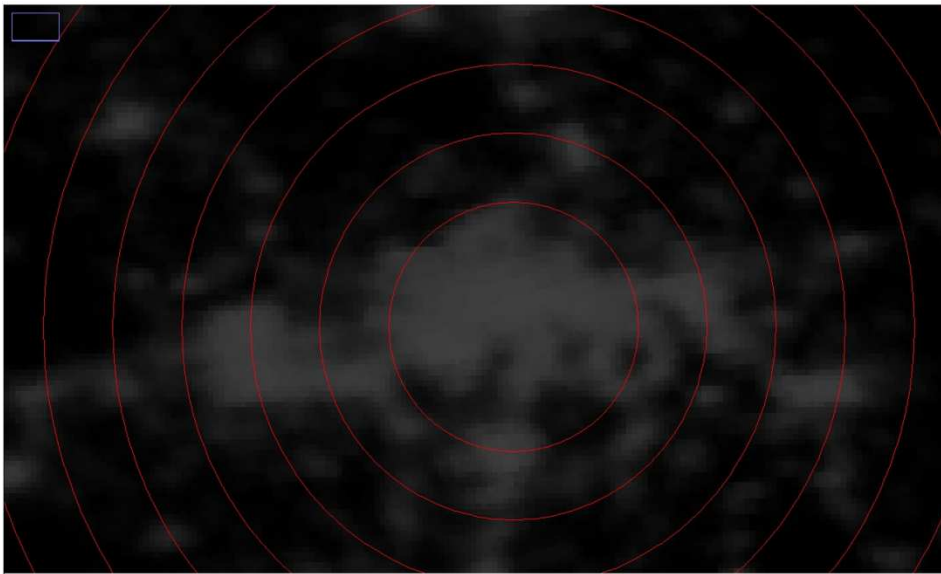
Frankfurt 1992
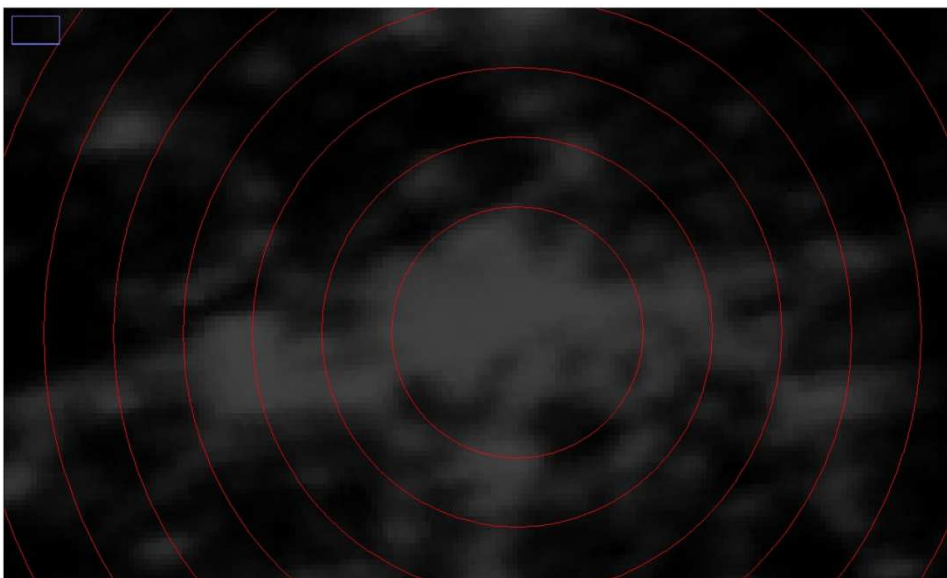
Frankfurt 2009

Descriptive statistics of the concentric circle analysis 1992

1992	Radius	Samples	Mean
1	23.300	189	31.772
2	36.167	293	18.867
3	49.033	397	10.443
4	61.900	497	7.748
5	74.767	601	2.564
6	87.633	705	1.670
7	100.500	805	0.389

18

Comparison 2009 versus 1992

2009 vs.1992	Radius	Samples	Mean	Difference	Mean diff.(%)
1	23.300	189	34.852	3.080	110
2	36.167	293	22.000	3.133	117
3	49.033	397	13.393	2.950	128
4	61.900	497	10.938	3.235	141
5	74.767	601	4.246	1.682	166
6	87.633	705	2.430	0.760	145
7	100.500	805	0.529	0.140	135
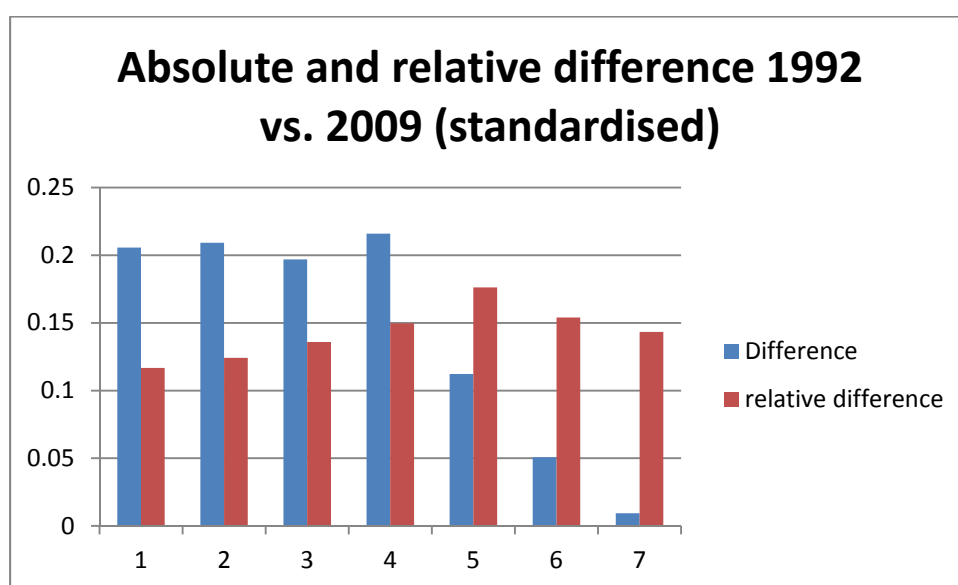
The 2nd and 4th circles are those with largest absolute increase of luminosity, while the 5th circle shows the largest relative increase. The 2nd circle represents parts of the outer peri-urban belt, while the 3rd and 4th circle cover mostly rural districts in the contiguous territory. Hence, rural areas, especially in the fourth circle have significantly integrated in the peri-urban landscape of Frankfurt and eventually the Rhein-Main area, as demonstrated by the spatial autocorrelation analysis for 2009 as compared to 1992:

Spatial autocorrelation: Moran-I Analysis 1992

	statistic	expected value	standard deviate	P-value[18]
Moran coefficient I	0.541	−0.167		
normality			2.081	0.037
randomisation			2.248	0.025

---

[18] Because of the little number of areas there is no meaningful significance test, so that here the *Moran I* coefficient can be only regarded as a descriptive correlation measurement. (Cf. Schulze 1995)

Spatial autocorrelation: Moran-I Analysis 2009

```
                       expected  standard
                 statistic  value   deviate  P-value

Moran coefficient I   0.563   -0.167
         normality                    2.145    0.032
         randomisation                2.223    0.026
```

There is an increase of *Moran's I* over time. Since there was no negative difference in luminosity between 1992 and 2009, spatial autocorrelation is supposed to be determined by increased agglomeration.[19]

There is one important caveat in this interpretation. Even though the Rhein-Main area is dominated by its urban center Frankfurt, the region is nevertheless rather characterized by a polycentric urban distribution with other major cities such as Wiesbaden, Mainz and Darmstadt. Hence, this agglomeration trend is not alone to be attributed to the pull-factor of Frankfurt.

A further local *Moran's I* analysis (LISA)[20] could shed more light on the changes of the local autocorrelation along the rings around the city. The following result tables are just to illustrate the method. The results on such a small number of observations are not sufficiently reliable. Among the significant coefficients compared, there is only an increase of *Moran's* local *I* for the second and the sixth ring and a slight reduction for the first ring.[21]

```
Moran's Ii (Mean DN)
-----------------------------------------------------------
          A | Ii      E(Ii)   sd(Ii)  z       p-value*
------------------+------------------------------------------
          3 | -0.001  -0.167   0.551   0.300   0.382
          4 |  0.099  -0.167   0.551   0.482   0.315
          5 |  0.415  -0.167   0.551   1.055   0.146
          7 |  0.807  -0.167   0.830   1.173   0.120
          6 |  0.720  -0.167   0.551   1.608   0.054
          2 |  0.805  -0.167   0.551   1.762   0.039
          1 |  1.613  -0.167   0.830   2.144   0.016
-----------------------------------------------------------
*1-tail test
```

Frankfurt 1992

```
Moran's Ii (Mean DN)
-----------------------------------------------------------
          A | Ii      E(Ii)   sd(Ii)  z       p-value*
------------------+------------------------------------------
          3 |  0.023  -0.167   0.562   0.337   0.368
          4 |  0.050  -0.167   0.562   0.385   0.350
          5 |  0.385  -0.167   0.562   0.982   0.163
          7 |  0.953  -0.167   0.853   1.312   0.095
          6 |  0.807  -0.167   0.562   1.733   0.042
          2 |  0.833  -0.167   0.562   1.779   0.038
          1 |  1.610  -0.167   0.853   2.082   0.019
-----------------------------------------------------------
*1-tail test
```

Frankfurt 2009

---

[19] Theoretically *Moran's I* could also increase if there is a negative trend of luminosity in all sections, with other words, when cities shrink or "ruralise". A decrease of *Moran's I* would happen if there are contrary trends in contiguous sections.

[20] A positive *Moran's* local *I* indicates an area with neighbours displaying similar value levels of a variable. A negative coefficient represents an outlier. Here the variable valued are highly dissimilar between two neighbouring areas. *Moran's* local *I* can only be properly interpreted under consideration of its z-score.

[21] The number of observations in this case is, however, too small to generate meaningful coefficients.

For an empirical analysis with *Moran's* local *I* one would need to increase the number of rings (minimum 30) to identify the geographical "breaks" of the coefficients along the rings. A shift of such breaks over time will indicate how areas have changed their functional relations.

9.2 Madrid

As a second example we have selected the agglomeration of Madrid. This agglomeration with around 7 million inhabitants is significantly larger than that of Frankfurt.

Descriptive statistics suggest a slightly more dynamic growth than that of Frankfurt. Mean pixel-DN increased from a similar level of 16.61 to 24.19 (e.g. a change of 45% versus 23% in the case of Frankfurt). Image correlation is thus also lower than in the case of Frankfurt.

Descriptive statistics

Image	Area	Mean	StdDev	Min	Max	IntDen
Madrid-F101992.v4b.avg_lights_x_pct.lzw-1.tif	18,832	16.61	19.47	0	63	312,715
MadridF162009.v4b.avg_lights_x_pct.lzw.tif	18,832	24.19	21.50	0	63	455,588

Image correlation 1992 vs. 2009

Pearson's_r
0.91

This we further examined by the radial profile analysis, another ImageJ plugin. The following two snapshots show the same section of Madrid agglomeration in 1992 and 2009. By visual inspection alone it becomes obvious that there is a considerably higher density of lights in 2009, revealing a process of urban growth.
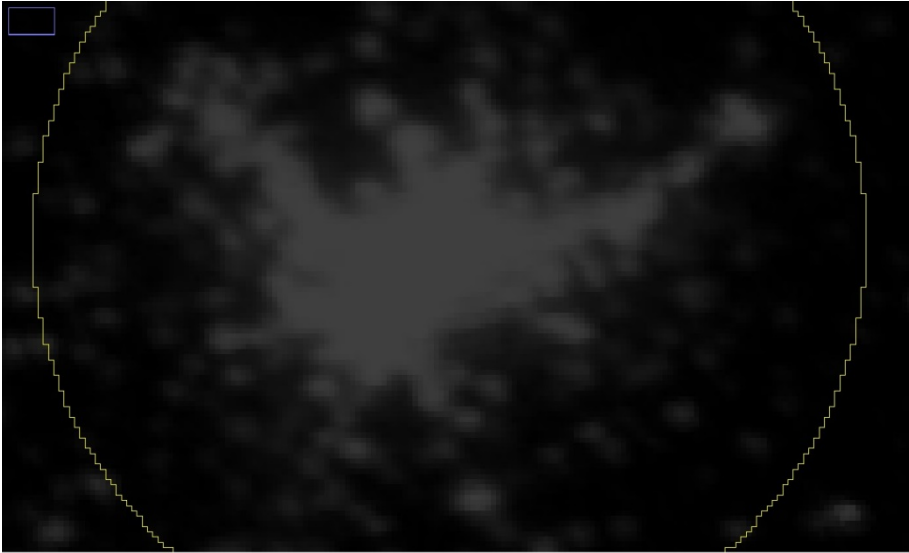
Madrid agglomeration 1992
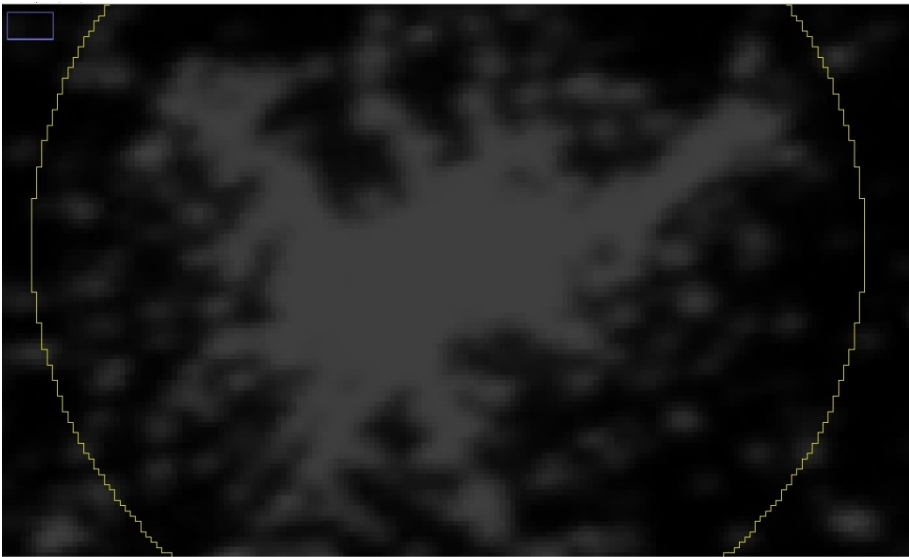
Madrid agglomeration 2009

The slope of the pixel distribution within the radial profile has significantly changed during 1992-2009 as shown by the following figures.[22]

---

[22] Normalised integrated intensity (Y): normalized by the average light intensity per pixel to sense pixel-to-pixel relative homogeneity
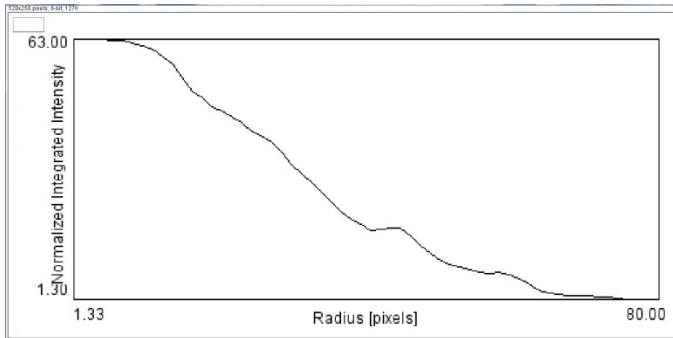
Madrid agglomeration 1992

```
OLS: y = a+bx
Sum of residuals squared: 1547.59839
Standard deviation: 5.12157
R²: 0.94784
Parameters:
       a = 64.87989
       b = -0.93758
```
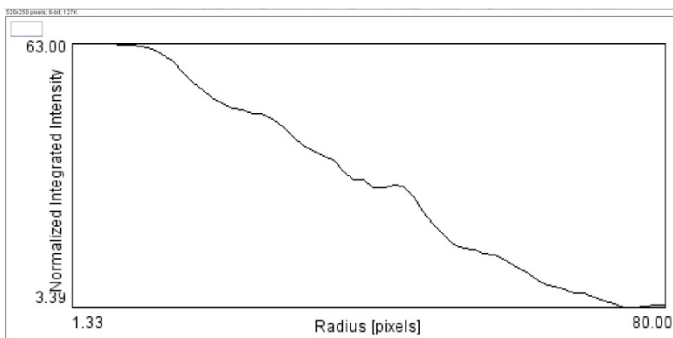

Madrid agglomeration 2009

```
OLS: y = a+bx
Sum of residuals squared: 360.71150
Standard deviation: 2.47260
R²: 0.98618
Parameters:
       a = 69.02228
       b = -0.89700
```

The above comparison of the same areal section shows a stronger trend to a linear relationship of radius and pixel density in 2009, while in 1992 the relation was more convex[23] revealing a decreasing marginal appearance of darker items (rural) along the radius from the

---

[23] showing the shape of f(x)<0 and f′(x)>0

inner to the outer sections. The 2009 image shows a slightly more balanced distribution of the pixel DN along the spectrum between 63 in the center and 0 in the outer areas, confirming that the agglomeration in the center has grown; therefore the linear best-fit line is better matched than that for the 1992 image. Consequently there was also a slightly weaker goodness of fit of the linear regression for 1992 ($R^2=0.95$) compared to that of 2009 ($R^2=0.99$).

Spatial autocorrelation: Moran-I Analysis

In a further analysis we again looked whether the city and its periphery has become more integrated during the 1992-2009 period and tested it with a simple spatial autocorrelation analysis, just as that demonstrated for Frankfurt.

First we ran an analysis with five circles within the limits of the radial extension analysed above[24]:

Analysis with five circles: 1992

	statistic	expected value	standard deviate	P-value
Moran coefficient I	0.472	−0.250		
normality			1.927	0.054
randomisation			1.868	0.062

Analysis with five circles: 2009

	statistic	expected value	standard deviate	P-value
Moran coefficient I	0.563	−0.250		
normality			2.168	0.030
randomisation			1.862	0.063

In contrast to Frankfurt there is a clearly stronger increase of spatial autocorrelation over time, even though in three cases the coefficients are insignificant. The density of light has increased in all circles, hence increased spatial autocorrelation is determined by further agglomeration during the 17 years.

The selection of size and number of circles is at the discretion of the researcher. In ImageJ the circles have the same radial distance. If selecting a small number of circles, there may be not only the problem of a too little number of observations but also misspecification, because areas of functional roles are not grouped around a city in constant distances (e.g. the *von Thunen* rings). However, when increasing the number of circles it becomes possible to compare different radial sizes of the rings, simply by adding up the moments of certain contiguous circles and calculating the mean pixel-DN. Then again it is possible to estimate spillovers by spatial autocorrelation.

---

[24] We waived inclusion of the two images and just report on the results.

We then tried an alternative estimation with 20 circles. The more neighbouring circles are compared the less variance between the sections is found, therefore spatial autocorrelation (*Moran's I*) with 20 circles is much higher, but still confirming increased autocorrelation during 1992 to 2009.

Alternative estimation with 20 circles: 1992

	statistic	expected value	standard deviate	P-value
Moran coefficient I	0.916	−0.053		
normality			4.457	0.000
randomisation			4.374	0.000

Alternative estimation with 20 circles: 2009

	statistic	expected value	standard deviate	P-value
Moran coefficient I	0.928	−0.053		
normality			4.513	0.000
randomisation			4.365	0.000

By merging certain rings of the 1992 image to indicate the different functional sections of the agglomeration, e.g. the rings 1 and 2 (city), 3 to 4 (outer metropolitan area), 5 to 7 (peri-urban ring), 8 to 11 (urban catchment area) and 12 to 20 (rural areas) it is possible to focus different sections in detail while adding up circles of sections of less interest to one circle. For example the selection city, outer metropolitan area, rings 5, 6 and 7, urban catchment area and rural areas will shed light on the change of the formerly peri-urban zone in 1992 and its change until 2009. With those seven selected rings the *Moran I* coefficient jumped from 0.57 in 1992 to 0.77 in 2009 revealing that formerly delineated functional zones have integrated into a more homogenous agglomeration area.

We then further increased the number of circles to 35 to test local spatial autocorrelation and its significance over time.
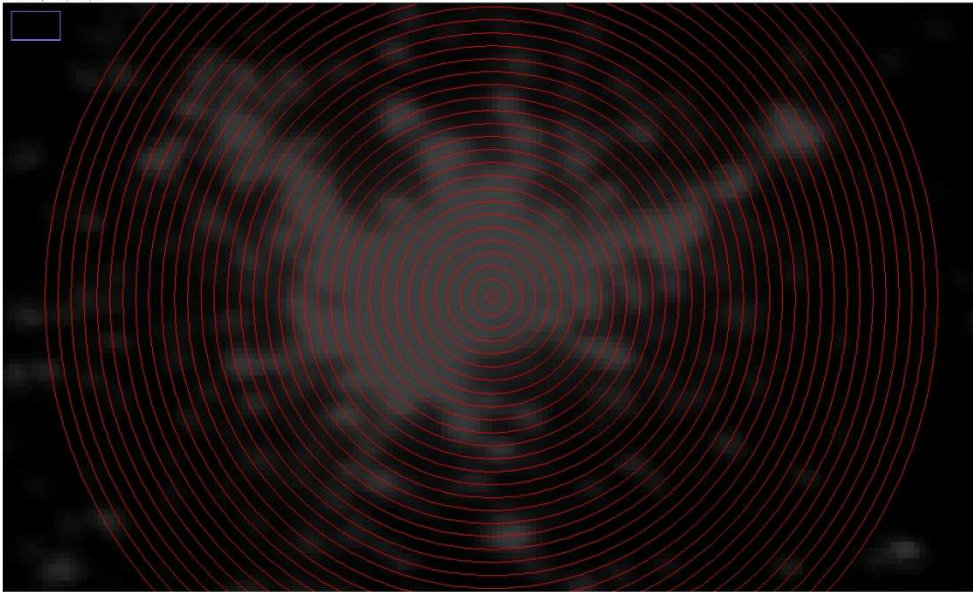
Madrid 1992: 35 circles
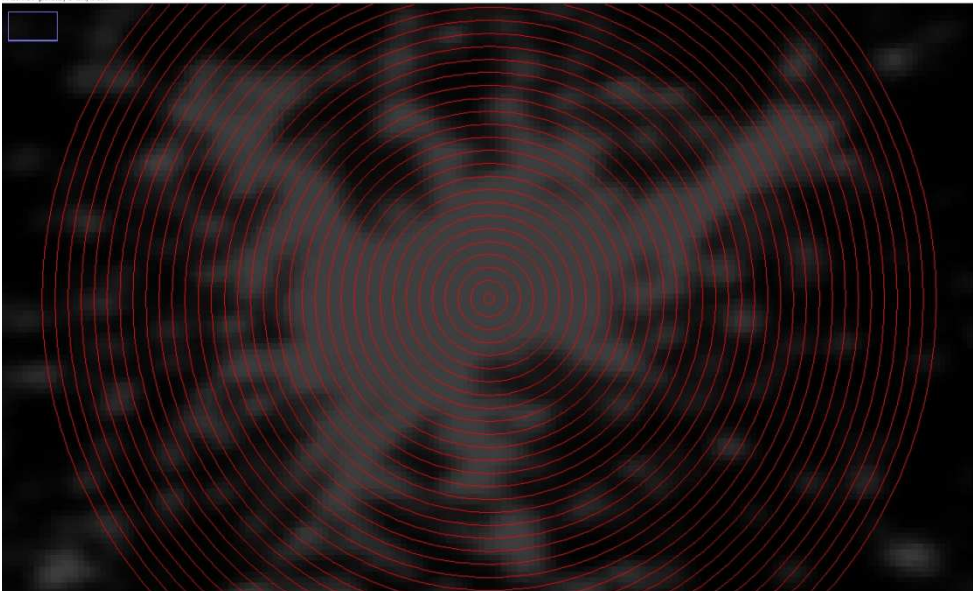
Madrid 2009: 35 circles

Based on the data we first looked at the global Moran's I that, as expected, shows a very strong (and equal) autocorrelation for both points of time. More interesting is exploring the change of local autocorrelation.

```
Moran's I
-----------------------------------------------------------------
        Variables |    I       E(I)    sd(I)     z     p-value*
------------------+----------------------------------------------
             Mean | 0.995   -0.029    0.171   5.990    0.000
-----------------------------------------------------------------
```
*1-tail test


```
Moran's Ii (Mean)
-----------------------------------------------------------------
           Circle |   Ii      E(Ii)   sd(Ii)     z     p-value*
------------------+----------------------------------------------
               15 | 0.003   -0.029    0.690   0.047    0.481
               16 | 0.004   -0.029    0.690   0.049    0.480
               17 | 0.026   -0.029    0.690   0.080    0.468
               14 | 0.044   -0.029    0.690   0.107    0.457
               18 | 0.075   -0.029    0.690   0.151    0.440
               13 | 0.151   -0.029    0.690   0.262    0.397
               19 | 0.160   -0.029    0.690   0.275    0.392
               20 | 0.237   -0.029    0.690   0.386    0.350
               21 | 0.298   -0.029    0.690   0.475    0.317
               12 | 0.345   -0.029    0.690   0.543    0.294
               22 | 0.377   -0.029    0.690   0.589    0.278
               23 | 0.483   -0.029    0.690   0.743    0.229
               11 | 0.587   -0.029    0.690   0.894    0.186
               24 | 0.624   -0.029    0.690   0.948    0.172
               25 | 0.779   -0.029    0.690   1.172    0.121
               10 | 0.841   -0.029    0.690   1.262    0.103
               26 | 0.876   -0.029    0.690   1.312    0.095
               27 | 0.911   -0.029    0.690   1.364    0.086
               35 | 1.351   -0.029    0.990   1.394    0.082
               28 | 0.945   -0.029    0.690   1.413    0.079
               29 | 1.015   -0.029    0.690   1.515    0.065
               30 | 1.129   -0.029    0.690   1.680    0.046
                9 | 1.130   -0.029    0.690   1.681    0.046
               31 | 1.245   -0.029    0.690   1.848    0.032
               32 | 1.320   -0.029    0.690   1.957    0.025
               33 | 1.356   -0.029    0.690   2.008    0.022
               34 | 1.358   -0.029    0.690   2.011    0.022
                8 | 1.375   -0.029    0.690   2.036    0.021
                7 | 1.517   -0.029    0.690   2.242    0.012
                6 | 1.713   -0.029    0.690   2.526    0.006
                1 | 2.794   -0.029    0.990   2.851    0.002
                5 | 2.054   -0.029    0.690   3.021    0.001
                4 | 2.375   -0.029    0.690   3.487    0.000
                3 | 2.582   -0.029    0.690   3.786    0.000
                2 | 2.731   -0.029    0.690   4.002    0.000
-----------------------------------------------------------------
```
*1-tail test
Madrid 1992: Spatial autocorrelation (35 circles)

```
Moran's I
----------------------------------------------------------------
        Variables |    I      E(I)    sd(I)    z     p-value*
------------------+---------------------------------------------
             Mean |  0.995  -0.029   0.171   5.983   0.000
----------------------------------------------------------------
*1-tail test
```

```
Moran's Ii (Mean)
----------------------------------------------------------------
           Circle |   Ii     E(Ii)   sd(Ii)    z     p-value*
------------------+---------------------------------------------
               17 |  0.001  -0.029   0.690   0.043   0.483
               18 |  0.001  -0.029   0.690   0.044   0.483
               16 |  0.009  -0.029   0.690   0.056   0.478
               19 |  0.011  -0.029   0.690   0.058   0.477
               20 |  0.038  -0.029   0.690   0.097   0.461
               15 |  0.049  -0.029   0.690   0.113   0.455
               21 |  0.083  -0.029   0.690   0.162   0.436
               14 |  0.136  -0.029   0.690   0.239   0.405
               22 |  0.149  -0.029   0.690   0.258   0.398
               23 |  0.258  -0.029   0.690   0.416   0.339
               13 |  0.264  -0.029   0.690   0.425   0.335
               12 |  0.438  -0.029   0.690   0.677   0.249
               24 |  0.459  -0.029   0.690   0.707   0.240
               11 |  0.659  -0.029   0.690   0.997   0.159
               25 |  0.732  -0.029   0.690   1.103   0.135
               10 |  0.933  -0.029   0.690   1.395   0.082
               26 |  0.975  -0.029   0.690   1.454   0.073
               27 |  1.125  -0.029   0.690   1.672   0.047
                9 |  1.187  -0.029   0.690   1.762   0.039
               28 |  1.193  -0.029   0.690   1.771   0.038
               29 |  1.273  -0.029   0.690   1.887   0.030
                8 |  1.292  -0.029   0.690   1.914   0.028
                7 |  1.315  -0.029   0.690   1.947   0.026
               35 |  1.972  -0.029   0.991   2.020   0.022
               30 |  1.451  -0.029   0.690   2.145   0.016
                6 |  1.457  -0.029   0.690   2.153   0.016
                1 |  2.107  -0.029   0.991   2.156   0.016
               31 |  1.653  -0.029   0.690   2.437   0.007
                5 |  1.762  -0.029   0.690   2.594   0.005
               32 |  1.798  -0.029   0.690   2.647   0.004
               33 |  1.900  -0.029   0.690   2.795   0.003
               34 |  1.958  -0.029   0.690   2.879   0.002
                4 |  1.999  -0.029   0.690   2.938   0.002
                3 |  2.075  -0.029   0.690   3.048   0.001
                2 |  2.100  -0.029   0.690   3.084   0.001
----------------------------------------------------------------
*1-tail test
```
*Madrid 2009: Spatial autocorrelation (35 circles)*

The above results show that there are more significant[25] coefficients in 2009 compared to 1992. In both years there is a significant local autocorrelation for the most inner circles and the most outer circles. Local *Moran*-I coefficients of the middle circles are insignificant. However, for 2009 there is an increase of significant coefficients in the range between the 27th and 30th ring, showing that areas in that distance to the central city become functionally more integrated, also confirmed by the shapes of the radial profile plots above.

A last simple but interesting tool of ImageJ is the Wand tool. With that instrument it is e.g. possible to view changes of the inner city or specific parts of the city by capturing the areas with identical pixel intensity. By using the 3-3-2 RGB filter and subsequently using the Wand tool, the boundaries of the city and the wider city are made visible. Moments of pixels can be

---

[25] By setting the threshold at $p=0.05$

calculated. The results show that the city area has grown strongly over the time, especially integrating the agglomeration along the Highway E-90 North-East (Torrejón de Ardoz to Guadalajara).
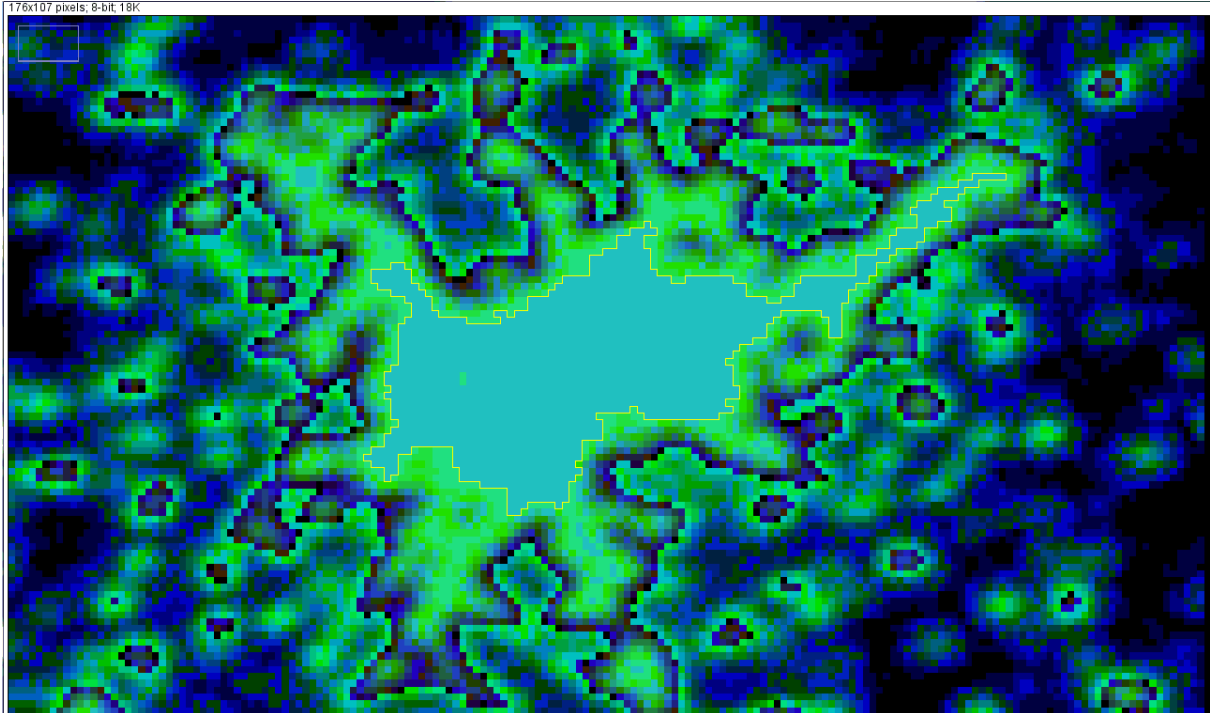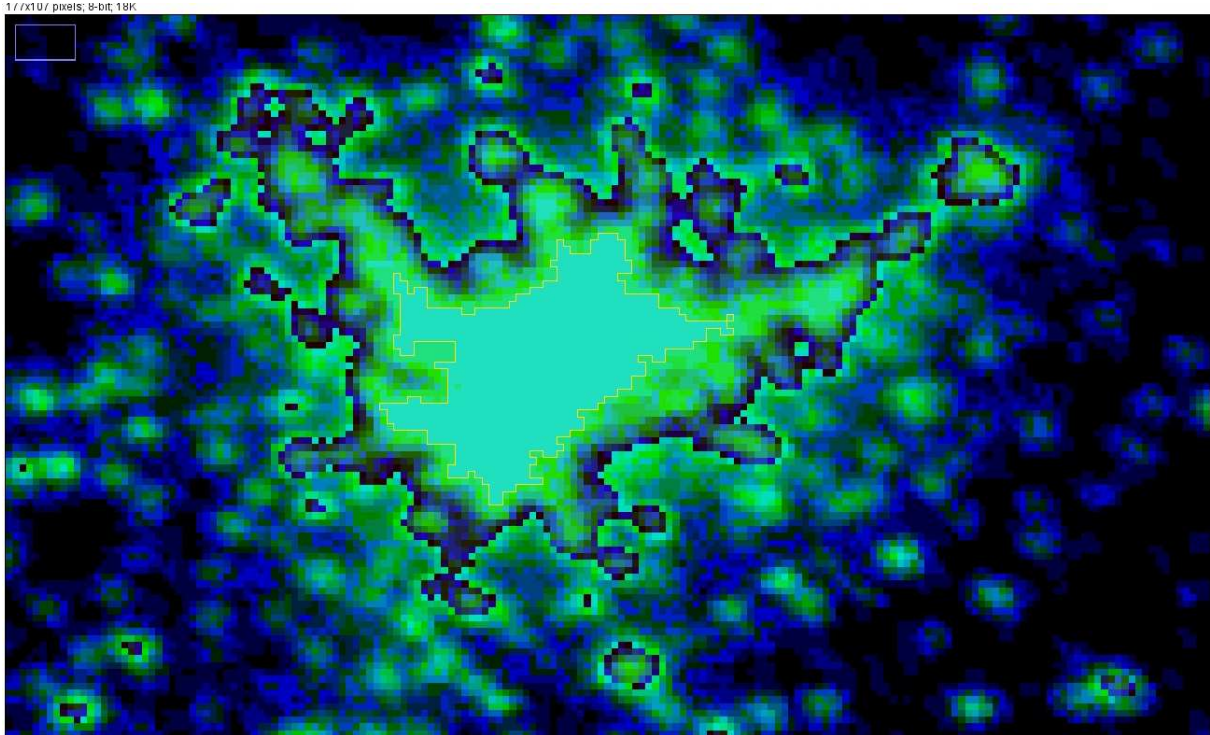
Growth of Madrid city 1992 vs. 2009

Label	Area	Mean	StdDev	Mode	Min	Max
Madrid-F101992.v4b.avg_lights_x_pct.lzw.tif	866	62.99885	0.03398	63	62	63
MadridF162009.v4b.avg_lights_x_pct.lzw.tif	1411	62.99858	0.03764	63	62	63

There are further analytic image analysis tools that could be tested for spatial analysis. Worth mentioning are fractal box counts, nearest neighbour analysis and others. In the final part of this paper we like to highlight a feature that is related to the deeper underlying order of spatial heterogeneity, namely the rank-size distribution of cities (or settlements respectively).

10. Spatial heterogeneity and Zipf's law

Further to the analysis of spatial dependence and the variation, scanning of night imagery can also be applied to analyses of spatial heterogeneity and to detect regular patterns of distribution. A well-known quasi-natural law of human settlement is the so-called rank-size distribution of cities. *Zipf's* law (Zipf 1949)[26] says that, at any country level, the largest city is x times larger than the city on rank x (measured on a logarithmic scale). Hence, based on empirical observations, the rank size distribution of cities is universally:

$$log(S) = c - q \, log(r) + u$$

where S means size of the city, c is a constant, r is the rank and the coefficient

$$q \approx 1$$

With *q*=1 the reverse relationship (*Pareto* distribution)

$$r = S^{-q}$$

would be equal, so it is possible to take both, *S* as well as *r* as the dependent variable or predictor respectively.

There is a large volume of research on *Zipf's* law, but this is overwhelmingly based on official data that is highly distorted by administrative boundaries, changes and error in official statistics. Such artificial boundaries – especially if they change – lead to major distortions of naturally delineated settlements. Thus there are also major deviations of validity of *Zipf's* law across countries and during time. Many observers thus have questioned the validity of *Zipf's* law.

Jiang et al. (2014) have used night satellite imagery to test *Zipf's* law globally. Luminosity is thus used as a proxy for settlements. The important advantage is that, with the data of light emission, there are neither administrative data restrictions nor do we need to acknowledge administrative boundaries. There is worldwide access to this variable. Furthermore it is possible to delineate functional settlements that make up "natural cities". A crucial point in this connection is the property of the *Pareto*-distribution, namely that there are many more small items than big ones and that the distribution of observations below and above the mean is rather skewed so that the mean as an expected value of a sample becomes
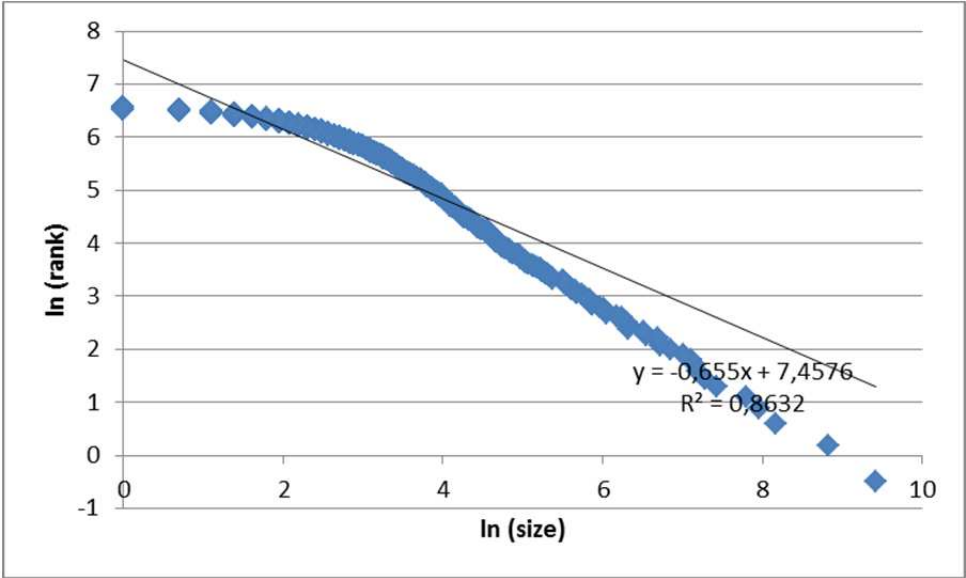
---

[26] *Zipf's* law is actually based on observations of Felix Auerbach in 1913 about patterns of population distribution. There are others before Zipf, such as Alfred Lotka or Frank Benford who have found similar relationships in other areas of life where observations are *pareto*-distributed.

meaningless.[27] However, the mean can be used to identify thresholds. It is possible to view the distribution of pixel intensity (DN) of a country or region and to find the mean DN. In subdividing the two parts (below and above the mean) into heads and tails and repeating this procedure for the observations for the respective head sections, the distribution becomes more and more linear, so that the procedure converges to a 50:50 distribution of observations below and above the mean. Settlements identified in this linear distribution are considered natural cities. Filtering-out pixel-DN being lower than their respective mean will then lead to a reduction of settlements that qualify as cities. Interestingly, the pattern of distribution of natural cities is significantly in line with *Zipf's* law, and this not only at country level but also at global and continental level. (Jiang 2015).

We tested this approach for Germany 2009 (within the area of 47.5° to 55.5° latitude and 6.5° to 14.5° longitude) with ImageJ

| Round	Pixels	Mean DN	Obs. Above mean	Obs. Below mean
1 (total)	689,984	11.55	32.3	67.7
2 (head)	222,869	27.76	41.6	58.4

First we ran a *Zipf* regression on the total 689,984 pixels with DN>0. The estimation of q was done with the *Gabaix-Ibragimov*-estimator[28] for the *Zipf* regression to reduce the bias in the standard OLS. Therefore we regressed rank on size instead size on rank. As we see, by viewing the total number of observations, the estimate for q differs strongly from the expected -1:


The chart shows a scatter plot of ln(rank) versus ln(size) with trendline $y = -0.655x + 7.4576$ and $R^2 = 0.8632$.

[27] For distributions with big tails (such as *Pareto*-, log-normal- or *Levy*- distributions) the central limit theorem does not hold.
[28] This coefficient is obtained by reducing the rank by ½ and then using the standard OLS approach, i.e. $ln\ (r-1/2)= c-q\ ln(S)$. The standard error of the Pareto exponent differs from the OLS standard error. It is asymptotically $(2/n)^{1/2}q$ (cf. Gabaix and Ibragimov 2007).

Following Jiang's approach to select a "natural" delineation of settlements we then filtered out any pixels lower than the threshold of DN 28 and could delineate settlements in the following map by ImageJ:
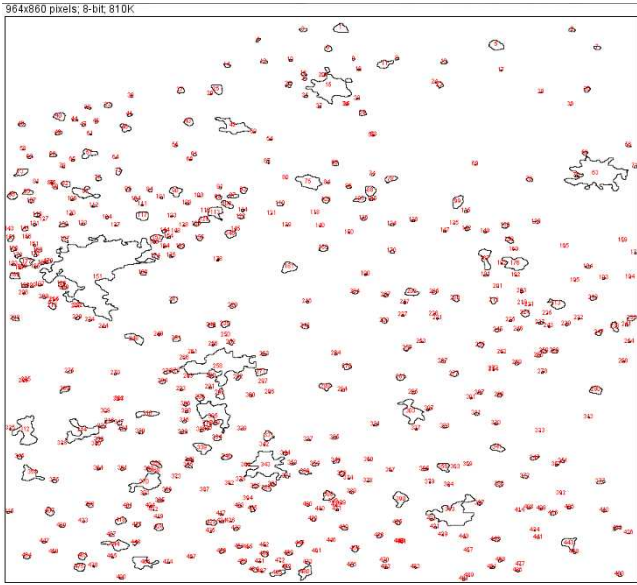
The subsequent *Zipf* regression led to the following result, which is significantly closer to the expected -1, with a nearly perfect goodness of fit:
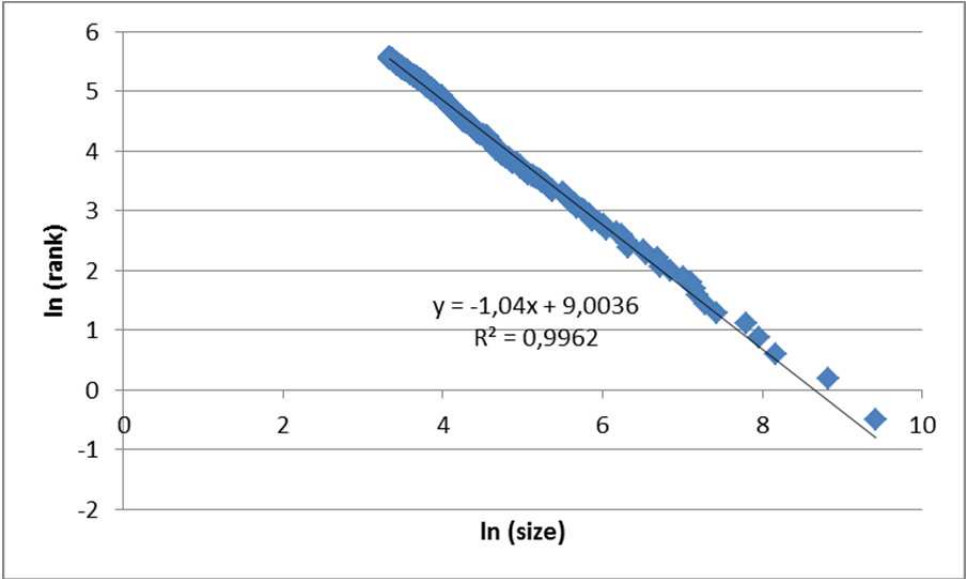
With a regression coefficient of -1.04, *Zipf's* law can be confirmed for the selected area.

Using the tool of night imagery it could be interesting to undertake further research on the behavior of the rank-size distribution of settlements among numerous different sizes and forms of selection of areas - within a country or for transnational regions, and to analyse the variation of *Zipf* coefficients among different shapes and sizes of areas selected.

11. Conclusion

The DMSP-OLS images and adequate image analysis software such as ImageJ (in some cases to be complemented by further statistics software) provide a useful perspective for the analysis of spatial change. Since there is a stable and significant correlation between social and economic variables (population density, GDP PPP) and luminosity, such image analyses contain important information on spatial economic development. Analysis of night imagery is certainly not adequate to replace the statistical analysis of regional data, but it is a good tool to confirm and illustrate patterns of spatial heterogeneity and spatial dependence over time.

Literature

Anselin, Luc 2001, "Spatial Econometrics", in: Baltagi, Badi H, *A Companion to Theoretical Econometrics*, Oxford: Blackwell

Auerbach, Felix 1913, „Das Gesetz der Bevölkerungskonzentration", *Petermanns Geographische Mitteilungen*, Vol. 59

Beck, Nathaniel, Kristian Skrede Gleditsch and Kyle Beardsley 2006, "Space is more than Geography: Using Spatial Econometrics in the Study of Political Economy", *International Studies Quarterly* Vol. 50

Berra, E, S. Gibson-Poole, A. MacArthur, R. Gaulton and A. Hamilton 2015, "Estimation of the spectral sensitivity functions of un-modified and modified commercial off-the-shelf digital cameras to enable their use as a multispectral imaging system for UAVs", *The International Archives of the Photogrammetry, Remote Sensing and Spatial Information Sciences*, Volume XL-1/W4

Buntilov, Vladimir M. 2013, "Pan-Sharpening of Multispectral Imagery Using Content-Specific Orthogonal Linear Transform", *International Journal of Computer and Communication Engineering*, Vol. 2/3

Chen, Xi and William D. Nordhaus 2011, "Using luminosity data as a proxy for economic statistics", *PNAS* Vol. 108/21

Coulter, Rory, Maarten van Ham and Allan M Findlay 2015, "Re-thinking residential mobility: Linking lives through time and space", *Progress in Human Geography* (forthcoming)

Damas, M.C., Vazgen Shekoyan, Paul Marchese, Tak Cheung 2014, *Comparative Fractal Analysis of 2013 November 5 Multiple Solar Eruptions with Fokker-Planck Equation Using Solar Dynamics Observatory Digital Images*, Proceedings ASEE 2014 Zone I Conference, April 3-5, 2014, University of Bridgeport

Doll, Christopher N.H. 2008, *CIESIN Thematic Guide to Night-time Light Remote Sensing and its Applications*, Palisades: Center for International Earth Science Information Network at Columbia University

Duranton, Gilles and Henry G. Overman 2002, *Testing for Localisation Using Micro-Geographic Data*, London: LSE

Gabaix, Xavier and Rustam Ibragimov 2007, *Rank-1/2: A simple way to improve the OLS estimation of tail exponents*, Cambridge: NBER

Ghosh, Tilottama, Rebecca L. Powell, Christopher D. Elvidge, Kimberly E. Baugh, Paul C. Sutton and Sharolyn Anderson 2010, "Shedding Light on the Global Distribution of Economic Activity", *The Open Geography Journal*, 2010/3

Halleck Vega, Solmaria and J. Paul Elhorst 2014, "Modelling regional labour market dynamics in space and time", *Papers in Regional Science*, Volume 93/4

Henderson, Vernon, Adam Storeygard, and David N. Weil 2011, "A Bright Idea for Measuring Economic Growth", *American Economic Review: Papers & Proceedings*, Vol. 101/3

Jiang, Bin 2014, "Geospatial Analysis Requires a Different Way of Thinking: The Problem of Spatial Heterogeneity", *Geojournal,* Januar 2014

Jiang, Bin, Junjun Yin, and Qingling Liu 2015, "Zipf's Law for All the Natural Cities around the World" *International Journal of Geographical Information Science*, Volume 29/3

Le Sage, James P. 1999, *The Theory and Practice of Spatial Econometrics*, Toledo: University of Toledo

Liu, Qingling 2014, *A Case Study on the Extraction of the Natural Cities from Nightlight Image of the United States of America*, Gävle: University of Gävle

Mellander, Charlotta, Kevin Stolarick, Zara Matheson and José Lobo 2013, *Night-Time Light Data: A Good Proxy Measure for Economic Activity?*, Toronto: Martin Prosperity Institute

Overman, Henry J. 2002, "Neighbourhood Effects in Large and Small Neighbourhoods", *Urban Studies*, Vol. 39, No. 1

Pinkovskiy, Maxim and Xavier Sala-i-Martin 2015, *Lights, Camera,…Income! Estimating Poverty Using National Accounts, Survey Means, and Lights*, Staff Report 669: Federal Reserve Bank of New York

Pinkovskiy, Maxim L. 2013, *Economic Discontinuities at Borders: Evidence from Satellite Data on Lights at Night*, Cambridge: MIT

Ramajo, Julián, Miguel A., Geoffrey J.D. Hewings, María M. Salinas 2008, "Spatial heterogeneity and interregional spillovers in the European Union: Do cohesion policies encourage convergence across regions?" *European Economic Review* Vol. 52 551–567

Schneider, Caroline A, Wayne S Rasband and Kevin W Eliceiri 2012, "NIH Image to ImageJ: 25 years of image analysis", *Nature Methods* Vol. 9/7

Schulze, Peter M. 1995, „Zur Messung räumlicher Autokorrelation", *Jahrbuch für Regionalwissenschaft*, Vol. 14

Sutton, Paul C., Christopher D. Elvidge and Tilottama Ghosh 2007, "Estimation of Gross Domestic Product at Sub-National Scales using Nighttime Satellite Imagery", *International Journal of Ecological Economics & Statistics* Vol. 8/S07

Troscianko, Jolyon and Martin Stevens 2015, "Image calibration and analysis toolbox – a free software suite for objectively measuring reflectance, colour and pattern", *Methods in Ecology and Evolution* 2015, 6

Ushizima, Daniela , Andrea G. C. Bianchi, Christina DeBianchi and E. Wes Bethel 2012, *Material Science Image Analysis using Quant-CT in ImageJ*, Berkeley: Lawrence Berkeley National Lab

van Woesik, Robert, Jessica Gilner, and Anthony J Hooten 2009, *Standard Operating Procedures for repeated measures of process and state variables of coral reef environments*, St. Lucia: Centre for Marine Studies, University of Queensland

Verhoeven, Geert, Christopher Sevara, Wilfried Karel, Camillo Ressl, Michael Doneus, and Christian Briese 2013, "Undistorting the Past: New Techniques for Orthorectification of Archaeological Aerial Frame Imagery", in: Corsi, C. et al. (eds.), *Good Practice in Archaeological Diagnostics*, Cham: Springer International Publishing

West, Jennifer L. and Ian D. Cameron 2011, "Using the medical image processing package, ImageJ, for astronomy", *The Journal of the Royal Astronomical Society of Canada* Vol 100/6

Whalley, J and S. Shanmuganathan 2013, *Applications of image processing in viticulture: A review*, Proceedings of the 20th International Congress on Modelling and Simulation, Adelaide, Australia, 1–6 December 2013

Zipf, George K. 1949, *Human Behaviour and the Principles of Least Effort*, New York: Addison Wesley

Zwiers, Merle, Gideon Bolt, Maarten van Ham and Ronald van Kempen 2014, *Neighborhood Decline and the Economic Crisis*, Bonn: IZA Discussion Paper